

SEPARATION OF σ_L AND σ_T IN η ELECTROPRODUCTION AT THE RESONANCE $S_{11}(1535)$

F.W. BRASSE, W. FLAUGER, J. GAYLER, V. GERHARDT, S.P. GOEL *,
C. GÖSSLING, R. HAIDAN, M. MERKWITZ, D. POECK and H. WRIEDT
Deutsches Elektronen-Synchrotron DESY, Hamburg, Germany

Received 28 March 1978

The ratio $R = \sigma_L/\sigma_T$ of longitudinal and transverse cross sections for the reaction $ep \rightarrow ep\eta$ at the resonance $S_{11}(1535)$ was measured at momentum transfers $q^2 = 0.6$ and 1 GeV^2 . The transverse part dominates the longitudinal part of the cross section. Averaging from $W = 1.49 \text{ GeV}$ to $W = 1.58 \text{ GeV}$ we obtain $R = 0.22 \pm 0.23$ at $q^2 = 0.6 \text{ GeV}^2$ and $R = -0.16 \pm 0.16$ at $q^2 = 1 \text{ GeV}^2$.

1. Introduction

It is one of the remarkable facts of electroproduction in the resonance region, that the electro-excitations of the two resonances $S_{11}(1535)$ and $D_{13}(1520)$ show different dependence on momentum transfer (q^2). The available data on $S_{11}(1535)$ electroproduction [1–3] and the total ep cross sections in that region [4] show that the electroproduction cross section of $S_{11}(1535)$ at $q^2 = 1 \text{ GeV}^2$ is reduced by at most 40% compared to its value at $q^2 = 0$, whereas $D_{13}(1520)$ is reduced by at least 70%. In principle the flat q^2 dependence of $S_{11}(1535)$ could be due to a significant contribution of σ_L which has to vanish at $q^2 = 0$.

Electroproduction of the resonance $S_{11}(1535)$ can be studied by the reaction $ep \rightarrow ep\eta$ which is a good indicator of $S_{11}(1535)$ due to the large branching ratio of the resonance into the decay channel ηp . All reported experiments on η production so far [1–3] took measurements at small electron scattering angles and at values of the polarization ϵ of the virtual exchanged photons around 0.9. These experiments therefore determined essentially the sum of σ_L and σ_T . It is the purpose of the present experiment to determine the ratio $R = \sigma_L/\sigma_T$ for η production in the region of $S_{11}(1535)$ by variation of the electron scattering angle. The measurements were done at momentum transfers $q^2 = 0.6$ and 1 GeV^2 where we had already performed detailed measurements at $\epsilon \approx 0.9$ [3]. The results given in this paper are numerically

* Now at Kurukshetra University, Kurukshetra, India.

somewhat different from those of ref. [13] due to an improved analysis [7] of the data.

2. Kinematics

We express the cross sections of the reaction $ep \rightarrow ep\eta$ in terms of the virtual photon absorption cross section $d\sigma/d\Omega^*$ in the C.M.S. of the final hadrons which is related to the differential coincidence cross section $d^5\sigma/dE'd\Omega_e d\Omega_\eta$ by

$$\frac{d^5\sigma}{dE'd\Omega_e d\Omega_\eta} = \Gamma_t \frac{d\sigma}{d\Omega^*} = \Gamma_t \left[\left(\frac{d\sigma}{d\Omega_\eta} \right)_T + \epsilon \left(\frac{d\sigma}{d\Omega_\eta} \right)_L \right]. \quad (1)$$

The photon flux factor Γ_t and the polarization ϵ of the transverse photons are defined as usual (see, e.g., ref. [5]).

If the assumption holds that in the final state only contributions of S-wave, interference of S-wave with P-wave, and P-wave with total angular momentum $\frac{1}{2}$ are present, the differential cross section can be described by [6]

$$\frac{d\sigma}{d\Omega^*} = A_0 + \epsilon B_0 + (A_1 + \epsilon B_1) \cos \theta^* + D_0 \sqrt{2\epsilon(\epsilon+1)} \sin \theta^* \cos \phi \quad (2)$$

The coefficients A_0 through D_0 are functions of W , the invariant mass of the final ηp system, and the momentum transfer q^2 only. The angles θ^* and ϕ are the c.m.s. polar and azimuthal production angles of the η meson (see fig. 1).

If the reaction proceeds *via* S-wave excitation, the cross section reduces to

$$\frac{d\sigma}{d\Omega^*} = A_0 + \epsilon B_0.$$

The ratio of longitudinal to transverse excitation is then given by

$$R = \sigma_L/\sigma_T = B_0/A_0.$$

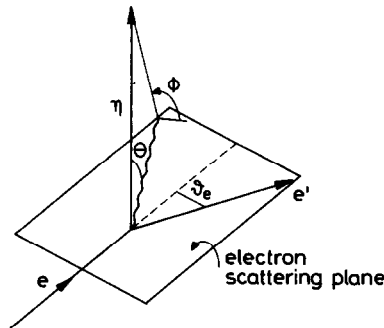


Fig. 1. Definition of angles.

We determined the dominating term $A_0 + \epsilon B_0$ and the two small terms $A_1 + \epsilon B_1$ and D_0 before at $\epsilon \approx 0.9$ for momentum transfers $q^2 = 0.6$ and 1 GeV^2 [3]. The present experiment partially repeats these measurements at $\epsilon = 0.9$ and determines σ_L by taking measurements in addition at $\epsilon \approx 0.5$.

3. Apparatus

The experimental set-up is described in more detail in ref. [3]. Only a short description is given here. The measurements are done in an external e^- beam of DESY. The primary beam hits a 12 cm liquid hydrogen target. The intensity is controlled by a secondary emission monitor, which was compared many times during the experiment to a Faraday cup. The scattered electron is detected in a focussing vertically bending spectrometer. It is identified by a threshold CO_2 Cerenkov and a sandwich shower counter. The horizontal angle ϑ_e of the spectrometer can be varied from 15° to 57° . A proton is detected in coincidence with the scattered e^- in a non-focussing spectrometer consisting of a vertically bending magnet, a system of proportional chambers mounted at the magnet exit, and a scintillator hodoscope. The trajectory is defined by the target and the intersections with the proportional chamber and the scintillator hodoscope. The horizontal angle of the proton spectrometer ϑ_p can be varied from 24° to 70° .

The apparatus stayed essentially unchanged when switching from the measurements at $\epsilon \approx 0.9$ to the measurements at $\epsilon \approx 0.5$. The only necessary changes besides the primary energy concerned the currents of the e^- spectrometer magnets and the horizontal angles of both spectrometers. The current of the proton spectrometer magnet remained unchanged. The data at $\epsilon \approx 0.9$ have been taken at $\vartheta_e = 15^\circ$ and $\vartheta_p = 34^\circ$, at $\epsilon \approx 0.5$ $\vartheta_e = 45^\circ$ and $\vartheta_p = 24^\circ$ were chosen.

The whole apparatus was tested at various times during the experiment by elastic ep coincidence measurements. As a further test the total ep cross section was measured continuously during the experiment. The results obtained are in reasonable agreement with the data of ref. [8].

4. Data analysis

The secondary electron and the recoiling proton are detected in coincidence. Protons are distinguished from π^+ mesons by time of flight [3]. The reaction $ep \rightarrow ep\eta$ is defined by the missing mass. The missing mass spectra at $\epsilon \approx 0.9$ in comparison to $\epsilon \approx 0.5$ are shown in fig. 2 at $W = 1.535 \text{ GeV}$.

Acceptances and various corrections have been calculated by a Monte Carlo simulation of the whole experiment. The W and q^2 dependence of η production used for the simulation was taken from ref. [3]. Radiation corrections have been incorporated into the Monte Carlo simulation, including internal and external radiation

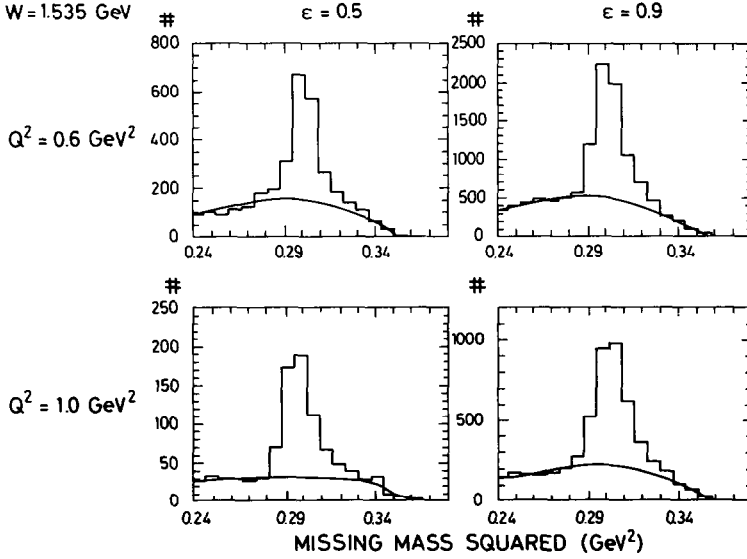


Fig. 2. Missing-mass spectra at $\epsilon = 0.5$ and $\epsilon = 0.9$ at $q^2 = 0.6$ and 1 GeV^2 , computed from the detected protons in coincidence with electrons. The data are from the range $1.52 < W < 1.55 \text{ GeV}$.

of the electrons. Also, a multipion background has been added according to a phase-space distribution. Experimental and Monte Carlo events were then analysed by the same program. The multipion background has been subtracted from the data by a fit to the events outside the η peak in the missing-mass distribution of each bin ($\Delta W = 30 \text{ MeV}$, $\Delta \cos \theta^* = 0.2$, $\Delta \Phi = 30^\circ$). The method is described in more detail in ref. [3].

The data are corrected for empty target rate (up to 1%), nuclear absorption ($\approx 1\%$), inefficiencies and multitrack events (up to 9%); random background (up to 14%) was subtracted.

5. Results

Due to the fact that the apparatus was kept essentially unchanged (see above), the angular acceptance stays the same at the settings with large and small ϵ ($-1 < \cos \theta^* < 1$, $15^\circ < \phi < 90^\circ$). Some examples of angular distributions are presented in fig. 3: A complete list of all measured differential cross sections will be given in ref. [7].

Fits according to eq. (2) to the individual distributions, at given ϵ and bin of W , show the dominance of the term $A_0 + \epsilon B_0$ as observed already in ref. [3].

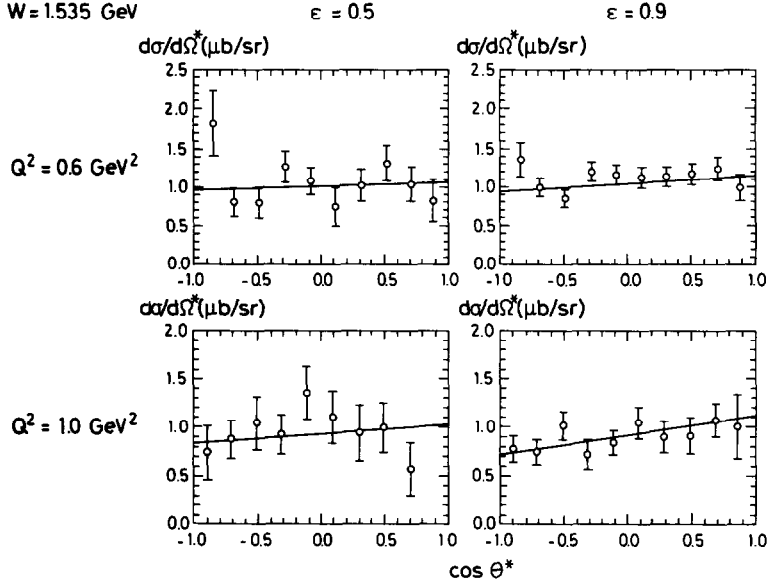


Fig. 3. Examples of angular distributions of $\gamma_{VP} \rightarrow \eta p$ at $W = 1.535$ GeV, $\phi = 60^\circ$. Solid line: fits according eq. (2) (see text).

Table 1
Angular coefficients of the reaction $\gamma_{VP} \rightarrow \eta p$.

q^2 [GeV ²]	W [MeV]	ϵ	$A_0 + \epsilon B_0$ [$\mu\text{b}/\text{sr}$]	$A_1 + \epsilon B_1$ [$\mu\text{b}/\text{sr}$]
0.62	1505	0.51	0.871 ± 0.081	0.132 ± 0.144
0.60	1505	0.91	0.954 ± 0.026	0.023 ± 0.044
0.59	1535	0.49	1.015 ± 0.056	0.048 ± 0.094
0.59	1535	0.90	1.055 ± 0.035	0.117 ± 0.061
0.56	1565	0.47	0.749 ± 0.066	-0.019 ± 0.120
0.58	1565	0.90	0.863 ± 0.039	-0.003 ± 0.064
0.57	1595	0.89	0.500 ± 0.039	-0.126 ± 0.068
1.02	1505	0.53	0.825 ± 0.078	0.168 ± 0.134
0.99	1505	0.92	0.715 ± 0.028	-0.030 ± 0.048
0.98	1535	0.52	0.920 ± 0.083	0.083 ± 0.140
0.98	1535	0.91	0.916 ± 0.041	0.204 ± 0.068
0.94	1565	0.50	0.716 ± 0.091	0.080 ± 0.159
0.97	1565	0.91	0.657 ± 0.034	0.006 ± 0.057
0.95	1595	0.91	0.441 ± 0.032	-0.052 ± 0.053
0.94	1625	0.90	0.348 ± 0.036	-0.098 ± 0.059

The quoted errors do not contain systematic errors of 6%.

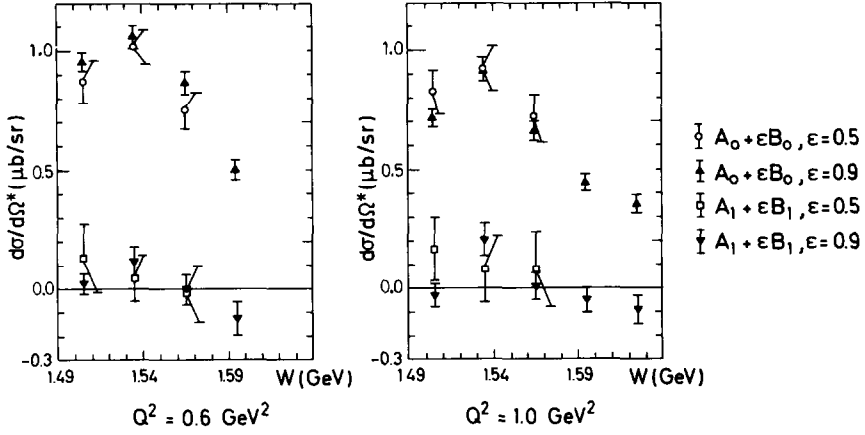


Fig. 4. Coefficients of angular distributions $A_0 + \epsilon B_0$ and $A_1 + \epsilon B_1$ as function of W at $q^2 = 0.6$ and 1.0 GeV^2 with $\epsilon = 0.5$ and $\epsilon = 0.9$.

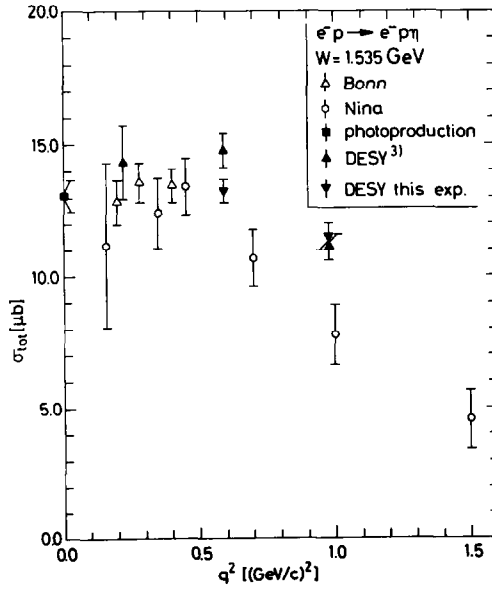


Fig. 5. Total cross section of $\gamma p p \rightarrow \eta p$ determined as $4\pi(A_0 + \epsilon B_0)$ at $\epsilon = 0.9$ and $W = 1.535 \text{ GeV}$ in comparison with former experiments. The point at $q^2 = 0$ has been obtained by averaging the results of ref. [10], corrected for the branching ratios of ref. [11].

Table 2

The ratio of longitudinal to transverse cross section $R = B_0/A_0$

W [GeV]	$R, q^2 = 0.6 \text{ GeV}^2$	$R, q^2 = 1 \text{ GeV}^2$
1.505	$0.27^{+0.52}_{-0.30}$	$-0.29^{+0.23}_{-0.15}$
1.535	$0.10^{+0.27}_{-0.19}$	$-0.01^{+0.36}_{-0.23}$
1.565	$0.43^{+0.57}_{-0.34}$	$-0.18^{+0.37}_{-0.21}$

The results given in table 1 and fig. 4 have been obtained keeping only $A_0 + \epsilon B_0$ and $A_1 + \epsilon B_1$ as free parameters in the fits according to eq. (2). Clearly the results are very similar at both values of ϵ , consequently σ_L must be small in η production. The integrated cross sections at $\epsilon \approx 0.9$ are in good agreement with our earlier results [3] (fig. 5). The DESY points in fig. 5 do not contain an estimated systematic error of 6%.

We determine the ratio of longitudinal to transverse production $R = B_0/A_0$ from the results on $A_0 + \epsilon B_0$ at the two values of ϵ . In table 2 and fig. 6 R is given as func-

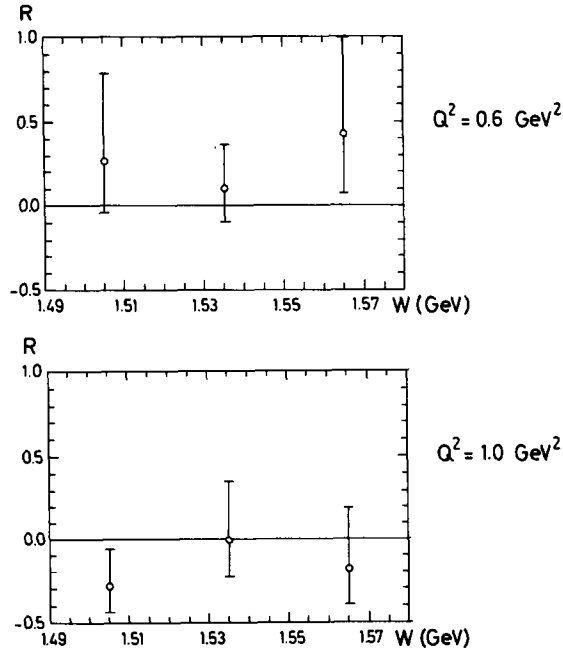


Fig. 6. Ratio of longitudinal to transverse η production $R = B_0/A_0$ as a function of W at $q^2 = 0.6$ and 1 GeV^2 .

tion of W at $q^2 = 0.6$ and 1 GeV^2 . The errors in table 2 and fig. 6 contain statistical and systematic errors. The latter result from our estimated uncertainty of 5% to measure the ratio of η production cross sections at $\epsilon \approx 0.9$ and $\epsilon \approx 0.5$.

Averaging over the whole accepted range of W from $W = 1.49 \text{ GeV}$ to $W = 1.58 \text{ GeV}$ we obtain $R = 0.22 \pm 0.23$ at $q^2 = 0.6 \text{ GeV}^2$ and $R = -0.16 \pm 0.16$ at $q^2 = 1 \text{ GeV}^2$. This compares well with a recently reported experimental result [12] $R = 0.16 \pm 0.10$ at $q^2 = 0.4 \text{ GeV}^2$. The multipole analysis of Devenish and Lyth [9] predicts R to be around 0.2 at $q^2 = 0.6 \text{ GeV}^2$ and around 0.12 at $q^2 = 1 \text{ GeV}^2$.

In conclusion, η production in the region of $S_{11}(1535)$ at $q^2 = 0.6$ and 1 GeV^2 has been found to be dominated by the transverse part of the cross section.

We gratefully acknowledge the excellent performance of the Synchrotron, the Hallendienst and the Rechenzentrum. We thank J. Koll, G. Singer, K. Thiele, H. Weiss and Mrs. H. Klement for careful technical work, and G. Wolf for reading the manuscript.

References

- [1] P.S. Kummer, E. Ashburner, F. Foster, G. Hughes, R. Siddle, J. Allison, B. Dickinson, E. Evangelides, M. Ibbotson, R.S. Lawson, R.S. Meaburn, H.E. Montgomery and W.J. Shuttleworth, *Phys. Rev. Lett.* 30 (1973) 873.
- [2] U. Beck, K.H. Becks, V. Burkert, J. Drees, B. Dresbach, B. Gerhardt, G. Knop, H. Kolanoski, M. Leenen, K. Moser, H. Müller, C.H. Nietzel, J. Päsler, K. Rith, M. Rosenberg, R. Sauerwein, E. Schlösser and H.E. Stier, *Phys. Lett.* 51B (1974) 103.
- [3] J.-C. Alder, F.W. Brasse, W. Fehrenbach, J. Gayler, R. Haidan, G. Glöe, S.P. Goel, V. Korbel, W. Krechlok, J. May, M. Merkwitz, R. Schmitz and W. Wagner, *Nucl. Phys.* B91 (1975) 386.
- [4] S. Stein et al., *Phys. Rev.* D12 (1975) 1884.
- [5] J.-C. Alder et al., *Nucl. Phys.* B46 (1972) 573.
- [6] C.W. Akerlof et al., *Phys. Rev. Lett.* 14 (1965) 1036.
- [7] H. Wriedt, Thesis, University of Hamburg, to be published.
- [8] F.W. Brasse et al., *Nucl. Phys.* B110 (1976) 413.
- [9] R.C.E. Devenish and D.H. Lyth, *Nucl. Phys.* B93 (1975) 169.
- [10] R. Prepost et al., *Phys. Rev. Lett.* 18 (1967) 82;
Cambridge Bubble Chamber Group, *Phys. Rev.* 169 (1968) 1081;
C. Bacci et al., *Phys. Rev. Lett.* 20 (1968) 571;
ABBHHM-Collaboration, *Phys. Rev.* 175 (1968) 1669;
E.D. Bloom et al., *Phys. Rev. Lett.* 21 (1968) 1100;
B. Delcourt et al., *Phys. Lett.* 29B (1969) 75;
E. Lehmann, Diplomarbeit, Hamburg, 1977;
- [11] Particle Data Group, *Rev. Mod. Phys.* 48 (1976) S1.
- [12] H. Breuker, V. Burkert, E. Ehses, W. Hillen, G. Knop, H. Kolanoski, M. Leenen, Ch. Nietzel, M. Rosenberg, A. Samel and R. Sauerwein, Paper 123 submitted to Int. Symp. on lepton and photon interactions at high energies, Hamburg, 1977.
- [13] F.W. Brasse et al., DESY 77/73 (1977).